



1 **Microbial carbon use for incorporating biomass phosphorus drives CO<sub>2</sub> emission**  
2 **in phosphorus-supplied subtropical forest soils**

3

4

5 Jianghao Tan <sup>1,3#</sup>, Muhammed Mustapha Ibrahim <sup>1#</sup>, Huiying Lin <sup>1,2</sup>, Zhaofeng Chang  
6 <sup>1,2</sup>, Conghui Guo <sup>1,2</sup>, Zhimin Li <sup>1</sup>, Xianzhen Luo <sup>1</sup>, Yongbiao Lin <sup>1</sup>, Enqing Hou <sup>1\*</sup>

7

8 <sup>1</sup> Guangdong Provincial Key Laboratory of Applied Botany & Key Laboratory of  
9 National Forestry and Grassland Administration on Plant Conservation and  
10 Utilization in Southern China, South China Botanical Garden, Chinese Academy of  
11 Sciences, Guangzhou 510650, China

12 <sup>2</sup> University of Chinese Academy of Sciences, 100039, Beijing, China

13 <sup>3</sup> Shanxi Agricultural University, Jinzhong 030801, China

14

15 # These authors contributed equally to this work

16 \* Corresponding author: [houeq@scbg.ac.cn](mailto:houe@scbg.ac.cn) (E. Hou).

17



18

### Abstract

19 Subtropical forests store significant amounts of soil organic carbon (SOC) and are  
20 important in the global C cycle. Current understandings based on controlled  
21 experiments indicate that phosphorus (P) availability promotes SOC decomposition  
22 by alleviating microbial P limitation or rendering SOC available for microbial  
23 decomposition. While no alternative mechanism is currently known, it is uncertain if  
24 this mechanism holds across soils or P supply levels at the field scale. We formulated  
25 an alternative mechanism for acidic subtropical forest soils where organic C (OC) is  
26 bound to iron (Fe). Our hypothesis proposed that P supply would promote Fe-bound P  
27 formation and desorption of OC previously bound to Fe, and the microbial utilization  
28 of the desorbed OC for P-cycling contributes significantly to CO<sub>2</sub> emission. We tested  
29 our hypotheses by utilizing a forest P addition platform to explore C-dynamics, its  
30 regulators, and utilization across four P supply levels: 0, 25, 50, and 100 kg P ha<sup>-1</sup> yr<sup>-1</sup>  
31 (Con, P1, P2, and P3, respectively) for one year. Phosphorus supply significantly  
32 increased the periodic and cumulative dissolved OC (DOC) concentration, especially  
33 in P3, and was associated with increased iron (Fe)-bound P formation. With increased  
34 DOC following P addition, microbial biomass P (MBP) significantly increased, while  
35 MBC remained unchanged. The significantly positive relationship between  
36 MBP:MBC ratio and DOC, significant increase in MBP and carbon dioxide (CO<sub>2</sub>)  
37 emission with P addition, and the reduction in CO<sub>2</sub> emission with increasing  
38 MBC:MBP ratio (0-10cm) supports our results that the desorbed-C alleviated  
39 microbial C-limitation induced during P-cycling, particularly, MBP incorporation, to  
40 drive CO<sub>2</sub> emission. Structural equation modeling and multivariate analyses projected  
41 MBP as a critical factor inducing CO<sub>2</sub> emission. Besides, insignificant alterations in  
42 the relative abundance of C-degrading functional genes and reductions in P- and C-



43 degrading enzyme activity indicated the sufficiency of desorbed OC for microbial use  
44 without further SOC degradation. Our study provides an alternative mechanism of P's  
45 impact on soil C-cycling processes in acidic subtropical forest soils vital for  
46 constraining process-based C models.

47

48 Keywords: phosphorus limitation, carbon turnover, subtropical forest, global change,  
49 acidic soils

50



## 51 **1. Introduction**

52 Forest soils are vital for carbon (C) storage in terrestrial ecosystems and store a  
53 significant proportion of soil organic C (SOC) (Slessarev et al., 2023). The SOC  
54 contains about twice the amount of the atmospheric C pool and about three times that  
55 of the terrestrial vegetation C pool; hence, small changes in its concentration will have  
56 a significant impact on atmospheric carbon dioxide (CO<sub>2</sub>) concentration and  
57 ecosystem C stock (Harris et al., 2021; Zheng et al., 2022). On the other hand,  
58 phosphorus (P) is an essential mineral nutrient for plant growth and regulates  
59 terrestrial vegetation productivity, soil microbial activity, biodiversity, and the C  
60 storage potential of soils (Hou et al., 2021). Recent studies have shown that soil total  
61 P concentration is highly spatially heterogeneous globally, ranging from 1.4 to 9636.0  
62 mg kg<sup>-1</sup> (He et al., 2021), and is significantly affected by soil and climatic factors  
63 (Hou et al., 2021). However, it is still unclear how the spatial heterogeneity in P  
64 affects SOC pools and their responses to global change, thus limiting our ability to  
65 predict SOC dynamics in the context of global change.

66 (Sub)tropical forests account for 61% of global tree cover by area (Wri, 2023)  
67 and, thus, play a central role in global C sequestration. The soils of these forests are  
68 highly weathered, have low pH, and are rich in reactive iron (Fe) phases. The  
69 chemical binding of reactive Fe to organic C in these soils is a key chemical  
70 mechanism for stabilizing SOC pools (Chen et al., 2022). Under acidic conditions,  
71 organic C is bound to Fe (Fe-OC) by adsorption and co-precipitation, making up  
72 about 37.8% of the total SOC in acidic forest soils (Zhao et al., 2016; Chen et al.,  
73 2020). Under these acidic soil conditions, P and organic C have a high affinity for Fe,  
74 resulting in competition for binding sites on Fe, and could be an obstacle to the  
75 formation of Fe-organic C complexes (Du et al., 2022), but reports on its influence on



76 Fe-organic C complexation remain under-explored in subtropical forests. Factors  
77 inducing the desorption of organic C would increase the soil dissolved organic C  
78 (DOC) pool, which constitutes a small fraction of the SOC pool but is the most active  
79 and bioavailable C source used to maintain the growth and metabolic activities of soil  
80 microorganisms (Liu et al., 2021). Hence, changes in soil DOC concentration can  
81 significantly affect the stability of SOC pools by regulating key soil processes such as  
82 soil microbial metabolism, nutrient turnover, and C mineralization (Tiwari et al.,  
83 2022). Given the importance of DOC in soil processes and microbial respiration,  
84 exploring the mechanisms regulating the effect of P supply on DOC and the  
85 underlying mechanisms is critical to accurately assess the stability of SOC in  
86 (sub)tropical forest soils.

87 Increased CO<sub>2</sub> emission and microbial biomass formation have been reported  
88 following P addition (Fisk et al., 2015; Liu et al., 2012), primarily associated with  
89 alleviating P limitation in microbes. Alternative mechanisms underlying this process  
90 remain unexplored. The potential desorption of organic compounds in soils following  
91 P addition (Du et al., 2022; Neff et al., 2000; Spohn et al., 2022) could provide more  
92 labile C and promote CO<sub>2</sub> emission. However, it is still unclear how P addition would  
93 impact SOC in conditions of higher Fe/Al oxides characterized by limited microbial  
94 activity, making it challenging to understand the dynamic of SOC in acidic conditions  
95 (Wordofa et al., 2019). Overall, considerable debate exists on how P supplies affect  
96 SOC pools across diverse ecosystems.

97 While many studies on the impacts of P on SOC in forest systems have been  
98 limited to the bulk SOC (Xia et al., 2024; Fang et al., 2019), other studies evaluated  
99 non-forest soils or used incubation studies without recourse to P supply levels or the  
100 impact of soil acidity (Spohn et al., 2022; Spohn and Schleuss, 2019). Changes in the



101 bulk SOC or short-term changes in organic C dynamics in non-forest soils provide  
102 limited information on the realistic impact of P supplies on forest SOC. Forest SOC is  
103 exposed to various biogeochemical alterations (e.g., atmospheric nitrogen deposition),  
104 with different turnover rates of its active pools (Trumbore, 2006). Besides, available  
105 studies did not evaluate the dynamic turnover of DOC by exploring the interactions  
106 between P, active Fe, and Fe-bound organic C in acidic subtropical forest soils.  
107 Therefore, the impact of P supply on SOC dynamics and DOC turnover and the  
108 underlying mechanisms remain unclear. Hence, a clearer insight into how P supplies  
109 alter active pools of SOC, especially DOC, in acidic forest soils and its mechanisms is  
110 important to improve SOC estimates of terrestrial ecosystem process-based models  
111 and combating climate change.

112 This study is based on the hypothesis that (i). P addition will compete with  
113 organic C for adsorption of active Fe, thereby promoting Fe-bound P and inducing the  
114 desorption of organic C previously bound to Fe in acidic subtropical forest soils (ii).  
115 Unlike the widely reported effect of P on promoting microbial C mineralization by  
116 relieving their P limitation, we hypothesized that the increased DOC induced by P  
117 addition in acidic soils would provide more labile C that drives microbial cycling of P  
118 to induce CO<sub>2</sub> emission. The key objectives of this study were to explore the response  
119 of organic C dynamics to soil P availability in acidic subtropical forest soils and to  
120 explore alternative mechanisms inducing increased CO<sub>2</sub> emission following P  
121 supplies.

122 Because the covariations in nitrogen (N), potassium (K), and other soil and  
123 climatic properties make it impossible to disentangle the impacts of P supply on SOC  
124 dynamics from the effects of other factors using natural P supply gradients, P addition



125 controlled experiments are vital to subdue these covariations to ensure accurate  
126 estimation of the impacts of P supplies on SOC dynamics.

## 127 **2. Methods**

### 128 **2.1. The study site**

129 The study was conducted at the Heshan Hilly Comprehensive Open Experiment  
130 Station of the Chinese Academy of Sciences. The station is located in the central part  
131 of Guangdong Province (112°54'E, 22°41'N) (Fig. S1) and is situated along the  
132 transition zone between tropical and subtropical climate. It has an average annual  
133 temperature and precipitation of 21.7 °C and 1700 mm, respectively, and the soil type  
134 is classified as latosol red soil (equivalent to Ultisol in the USDA soil classification  
135 system). The project site is an evergreen, broad-leaved mixed forest of about 0.5  
136 hectares planted in 1984. The main tree species are *Cinus glauca*, *Mucuna pruriens*,  
137 and *Schima superba*.

### 138 **2.2. Plot settings**

139 The experimental platform was set up in June 2022 and comprises four levels of P  
140 and K additions (0, 25, 50, and 100 kg ha<sup>-1</sup> yr<sup>-1</sup>). For our study, we selected the plots  
141 with P addition from the research platform comprising four treatments: the control (no  
142 P) and different levels of P addition (P1: +25 kg P ha<sup>-1</sup> yr<sup>-1</sup>, P2: +50 kg P ha<sup>-1</sup> yr<sup>-1</sup>,  
143 and P3: +100 kg P ha<sup>-1</sup> yr<sup>-1</sup>). The basic nutrient concentration of the plots was  
144 obtained before establishing the experiment. Each plot is demarcated by PVC panels  
145 installed 30 cm above and below the ground, with a buffer zone of 2-5 m between  
146 plots (Fig. S1). Each treatment was set with three replicates, with a total of 12



147 quadrants of  $10 \times 10 \text{ m}^2$  (Fig. S1). Two static field-based chambers were installed per  
148 plot (Fig. S1) for the monthly measurement of  $\text{CO}_2$  emissions following P addition.

### 149 ***2.2.1. Phosphorus addition***

150 Analytical grade sodium dihydrogen phosphate ( $\text{NaH}_2\text{PO}_4$ ) was used as the P  
151 source. It was dissolved in water to form a solution and applied according to the P rate  
152 specified for each treatment. The P addition rate was applied as a one-time, complete  
153 dose application evenly sprayed per plot in the form of understory spraying.  
154 Phosphorus was added using 20 L of P-dissolved water per quadrant with a back-  
155 mounted knapsack sprayer to ensure uniform distribution. The same amount of tap  
156 water was sprayed in the control treatment to eliminate possible differences between  
157 treatments due to the added water during P addition across the P addition treatments.

### 158 ***2.3. Samples collection and processing***

159 In each quadrant, 0-10 cm and 10-20 cm mineral soil samples were collected  
160 (after removal of surface organic materials) after 2 weeks, 1, 2, 4, 6, 8, 10, and 12  
161 months after P addition. Three cores per depth were collected in each plot and bulked  
162 to form composite samples. Soil sampling was limited to the top 20 cm mineral depth  
163 because it is the region with the most active biochemical reactions and microbial  
164 activity that can significantly impact our investigation. Litterfall (from understory and  
165 overstory plants) was collected monthly during the one year using two  $1 \text{ m}^2$  meshes  
166 raised along the central region of each plot (Fig. S1). Forest floor litter was collected  
167 at 6-month intervals per plot, weighed, oven-dried, and analyzed for DOC  
168 concentration.





169 The fresh soil samples per depth (per plot) were well-mixed and passed through a  
170 2 mm sieve to remove fine roots and stones. Some soil samples were stored at 4 °C for  
171 the analysis of soil microbial biomass and enzyme activity, while the other portion  
172 was stored at -80 °C for subsequent DNA extraction and next-generation sequencing  
173 of microbial functional genes. The remaining samples were air-dried and analyzed for  
174 soil Fe concentration and C and P components.

#### 175 ***2.4. Soil CO<sub>2</sub> measurement***

176 The static chambers shown in Fig. S1 were used to collect monthly gas  
177 samples, which were transferred into gas sampling bags. The gas samples were  
178 collected at 30-minute intervals from the chambers pre-installed on the field. The CO<sub>2</sub>  
179 concentration in each sample was analyzed using a gas chromatography (GC) system  
180 (Agilent 7820A, Santa Clara, CA, U.S.) (within 1-2 days after collection), and the  
181 values obtained were used to calculate the soil's CO<sub>2</sub> emission rate. Soil temperature  
182 and moisture content were measured simultaneously during gas sample collection  
183 using soil-installed thermo-hygrometer sensors.

#### 184 ***2.5 Samples analyses***

185 The soil pH value was measured using a water-to-soil ratio of 1:2.5 using a pH  
186 meter. The active Fe components in the soil were obtained by extracting free Fe-oxide  
187 with dithionite–citrate–bicarbonate solution, representing both crystalline and non-  
188 crystalline Fe oxides. The modified Hedley fractionation method (Hou et al., 2018)  
189 was used for the sequential extraction of P fractions into different groups with varying  
190 availability (resin Pi, NaHCO<sub>3</sub> Pi, NaHCO<sub>3</sub> Po, NaOH Pi, NaOH Po, HCl Pi, residual  
191 Pi, residual Po, and total P) to obtain the Fe-bound P represented by the NaOH Pi. The



192 NaOHPI was used to represent the Fe-bound P because, aside from Al, the Fe-bound P  
193 dominates the inorganic P extracted by NaOH (Hou et al., 2014). Soil available P  
194 concentration was determined using the malachite-green method (Ohno and Zibilske,  
195 1991) and read on a spectrophotometer (UV-3802H, UNICO, Shanghai, China) at a  
196 wavelength of 640 nm. The DOC in soil and litter was measured using the cold water  
197 method extraction at a water:soil ratio of 1:4 and read on a TC/TN analyzer  
198 (Shimadzu TOC-V CPH, Japan). The amount of DOC extracted from the soil samples  
199 was used as a proxy for the C desorbed following P addition based on the description  
200 of Spohn and Schleuss (2019).

201 Enzymes that catalyze the degradation of organic carbon ( $\beta$ -1,4-glucosidase  
202 [BG]) and phosphorus (acid phosphatase [AP]) were quantified with fluorometric  
203 assays following the protocol developed by Bell et al. (Bell et al., 2013) using 2.75 g  
204 of fresh soil. Microbial biomass C (MBC) and microbial biomass P (MBP) were  
205 determined following soil fumigation with alcohol-free chloroform for 24 h (Vance et  
206 al., 1987). The extraction and measurement of soil MBC was done using 0.5 M  $K_2SO_4$ ,  
207 while the MBP was extracted using the malachite green method described for the soil  
208 available P.

209 To explore the dynamics of functional genes mediating organic C degradation  
210 and utilization, soil genome-wide DNA extraction and next-generation high-  
211 throughput sequencing were carried out in fresh soils collected from the 0-10 cm soil  
212 depth. The Mag-Bind® Soil DNA Kit (Omega Bio-tek, Norcross, GA, U.S.) was used  
213 for DNA extraction based on the manufacturer's protocols. The concentration and  
214 purity of extracted DNA were determined with TBS-380 and NanoDrop2000,  
215 respectively. The quality of the DNA extract was checked on 1% agarose gel. The  
216 extracted DNA was fragmented to an average size of about 400 bp using Covaris



217 M220 (Gene Company Limited, China) for paired-end library construction using  
218 NEXTFLEX Rapid DNA-Seq (Bioo Scientific, Austin, TX, USA). Paired-end  
219 sequencing was performed on Illumina NovaSeq (Illumina Inc., San Diego, CA, USA)  
220 at Majorbio Bio-Pharm Technology Co., Ltd. (Shanghai, China) using the NovaSeq  
221 6000 S4 Reagent Kit v1.5 (300 cycles) according to the manufacturer's instructions.

## 222 **2.6 Data processing and analyses**

223 Analysis of variance was used to statistically test the differences in the measured  
224 parameters among the treatments and sampling times. The relationship between DOC,  
225 CO<sub>2</sub> flux, and C and P components with P availability was established using structural  
226 equation modeling (SEM) with the *sem* package in R. Unlike the traditional  
227 correlation analysis, SEM allows for variables to serve as responses on one path and  
228 as predictors on another, making it useful for testing and quantifying indirect or  
229 cascading effects of P availability on soil C and P components and CO<sub>2</sub> emission. We  
230 further used the Mantel test to explore the spatial autocorrelation between soil  
231 properties, CO<sub>2</sub> emission, C and P components and their functional genes. All  
232 analyses were conducted using the R software (v4.3.2) and OriginPro (v2021).

233 The raw data obtained from high-throughput sequencing was processed using the  
234 free online platform of Majorbio Cloud Platform ([www.majorbio.com](http://www.majorbio.com)). fastp  
235 (<https://github.com/OpenGene/fastp>, version 0.20.0) was utilized for adapter trimming  
236 and removing sequences with low quality (quality threshold value < 20 and length <  
237 250 bp). Metagenomics data were assembled using MEGAHIT (version 1.2.9) (Li et  
238 al., 2015) with default k-mers. Contigs with lengths  $\geq 300$  bp were selected as the  
239 final assembly result and used for further gene prediction and annotation. The  
240 expression of the functional genes regulating C and P cycling was measured using

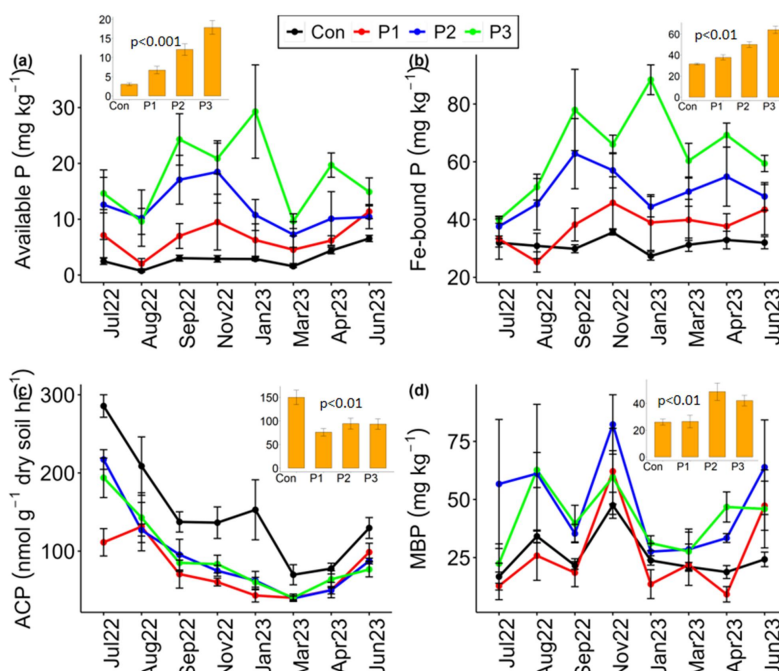


241 their relative abundance, which was normalized to transcript per million (TPM) based  
242 on the gene length and sequencing depth (based on the Kyoto Encyclopedia of Genes  
243 and Genomes (KEGG) Orthology-knockout (KO)) and quantified using Salmon  
244 v1.5.182). The alpha diversity of total bacterial functional genes was evaluated using  
245 the number of observed species (Sobs), Chao1, the Abundance-based Coverage  
246 Estimator (ACE), Shannon, and Simpson's indexes. Redundancy analysis (RDA) was  
247 conducted to establish the constrained relationship between soil P and C components  
248 and their influence on C and P cycling genes and CO<sub>2</sub> emission.

### 249 **3. Results**

#### 250 **3.1. Responses of soil phosphorus and carbon to phosphorus supplies**

251 Over one year, a one-time supply of increasing P across the experimental plots  
252 consistently increased the cumulative concentration of available P (Figs. 1a, S2a)  
253 while increasing the P bound to Fe in the soil (Fig. 1b), particularly in the 0-10 cm  
254 depth. A similar pattern was observed in the 10-20 cm depth (Fig. S2b). While acid  
255 phosphatase decreased with P supply across both depths (Figs. 1c, S2c), microbial  
256 biomass P (MBP) significantly increased with P supplies, particularly at P2 and P3  
257 (Figs. 1d, S2d).



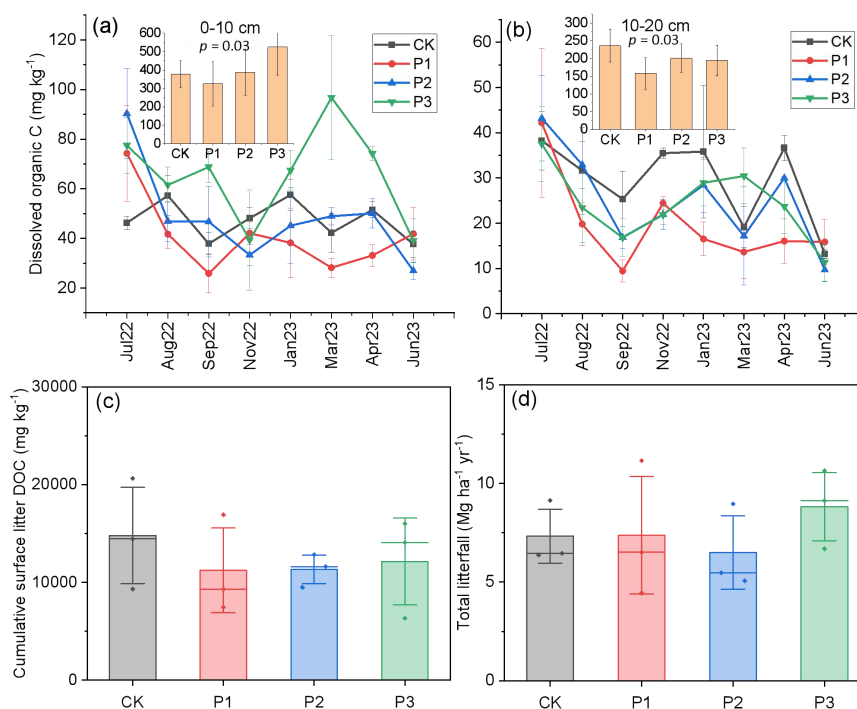
258  
259 **Fig. 1.** Repeated measures of soil P dynamics over one year after phosphorus (P)  
260 additions in the 0-10 cm depth. a. available P concentration extracted by Bray-1  
261 method, b. iron-bound P (NaOH Pi) concentration, c. acid phosphatase activity, and d.  
262 microbial biomass P concentration. Each line/bar represents the mean value of each  
263 treatment (n=3 (lines), n=24 (bars),  $p < 0.05$ ). The error bars represent the standard  
264 error of the mean. MBP: microbial biomass P, ACP: acid phosphatase. Con: control,  
265 P1: 25 kg P ha<sup>-1</sup>, P2: 50 kg P ha<sup>-1</sup>, P3: 100 kg P ha<sup>-1</sup>.

266  
267  
268

269 Across the different sampling times, there was a significant increase in the  
270 concentration of DOC with increasing P supply, particularly in the P3 treatment (Fig.  
271 2a). Thus, after one year, there was a significant difference ( $p = 0.03$ ) in the  
272 cumulative concentration of DOC among the treatments, with the highest value  
273 obtained in the P3 treatment. However, the increase in DOC with P supply was  
274 limited to the 0-10 cm depth as a significant reduction ( $p = 0.03$ ) in DOC was  
275 recorded with P addition compared to the control (Fig. 2b). The cumulative surface  
litter DOC concentration did not significantly vary across the treatments (Fig. 2c).



276 Similarly, the cumulative total litterfall amount, which could contribute to DOC after  
277 decomposition did not vary with P addition levels (Fig. 2d).  
278



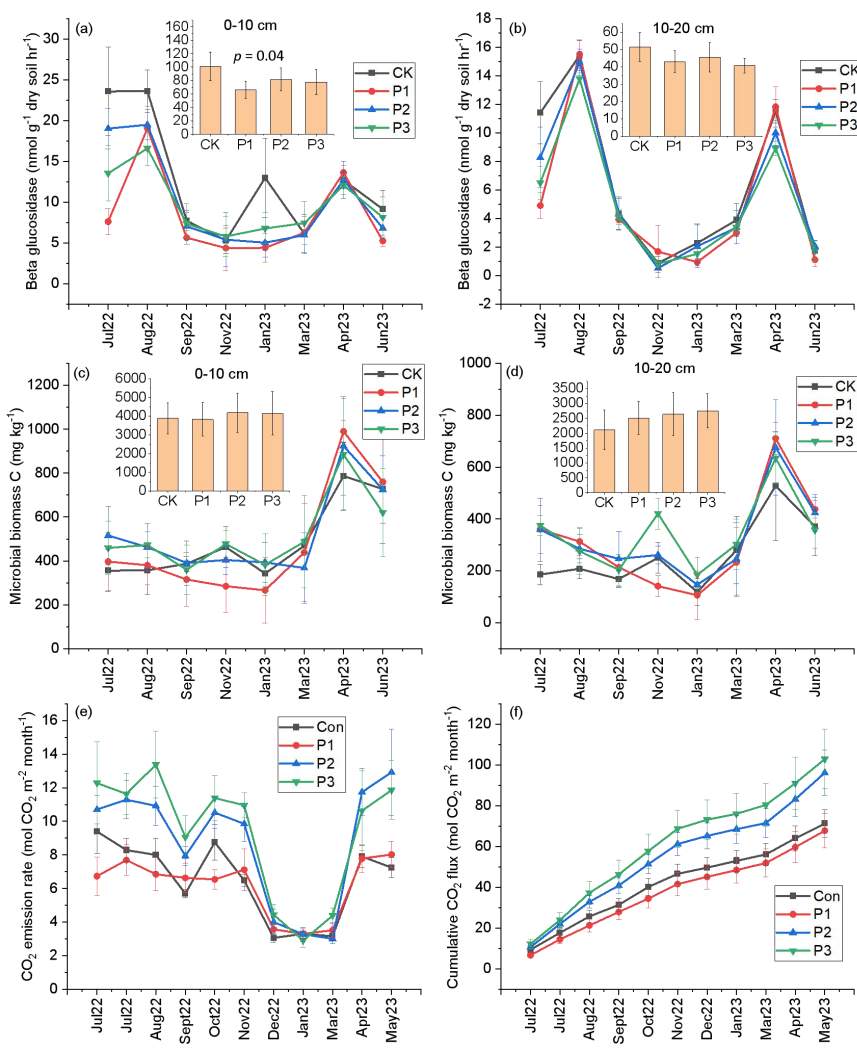
279 **Fig. 2.** Dynamics of dissolved organic carbon (C) in soil, surface litter, and litterfall  
280 quantity with increasing P supply. a. dissolved organic C in the 0-10 cm depth, b.  
281 dissolved organic C in the 10-20 cm depth, c. cumulative dissolved organic C in the  
282 surface litter, d. cumulative plant litter biomass. Each line/bar represents the mean  
283 value of each treatment (n=3 (lines), n=24 (bars),  $p < 0.05$ ). The error bars represent  
284 the standard error of the mean, using Tukey's test (n=24,  $p < 0.05$ ). CK: control, P1:  
285 25 kg P ha<sup>-1</sup>, P2: 50 kg P ha<sup>-1</sup>, P3: 100 kg P ha<sup>-1</sup>.  
286

287  
288 The beta-glucosidase activity, which is involved in the breakdown of organic  
289 C to release glucose for microbial use, was cumulatively significantly reduced ( $p =$   
290 0.04) after P addition compared to the control treatment, but without variation among  
291 the P addition rates in the 0-10 cm depth (Fig. 3a). Such a reducing trend, while not  
292 significant was observed in the lower 10-20 cm depth (Fig. 3b). The amount of C



293 stored in the microbial biomass did not significantly vary among the control and P  
294 addition both in the 0-10 and 10-20 cm soil depth (Fig. 3c and d). Across the 0-10 and  
295 10-20 cm depth, the concentration of non-crystalline Fe in the soil showed an  
296 increasing trend with P addition across the sampling times and cumulatively over a  
297 year, with higher values obtained in P2 (Fig. S3a-d).

298 Monthly measurements of CO<sub>2</sub> emission reveal a consistent increase in CO<sub>2</sub>  
299 flux with higher P supplies, particularly in P2 and P3 (Fig. 3e). CO<sub>2</sub> flux was  
300 significantly lowest and did not vary among treatments during the cold periods (from  
301 December to March) (Fig. S4a) and during months with reduced precipitation (Fig.  
302 S4b). There was a significant ( $p = 0.02$ ) difference in the cumulative CO<sub>2</sub> emission  
303 among the treatments, with the highest mean values recorded in P2 and P3 (40.7 and  
304 43.9  $\mu\text{mol CO}_2 \text{ m}^{-2} \text{ s}^{-1}$ , respectively), compared to the control (30.1  $\mu\text{mol CO}_2 \text{ m}^{-2} \text{ s}^{-1}$ )  
305 and the P1 treatment (28.7  $\mu\text{mol CO}_2 \text{ m}^{-2} \text{ s}^{-1}$ ) (Fig. 3f).



306  
 307 **Fig. 3.** Dynamics microbial carbon (C) cycling with increasing phosphorus supply.  
 308 Beta-glucosidase activity in the a. 0-10 cm depth, b. 10-20 cm depth. c. microbial  
 309 biomass C in the 0-10 cm depth, d. in the 10-20 cm depth, e. monthly CO<sub>2</sub> emission  
 310 across sampling times, and f. cumulative CO<sub>2</sub> flux over one year. Each line/bar  
 311 represents the mean value of each treatment (n = 3 (lines), n = 24 (bars), p < 0.05).  
 312 The error bars represent the standard error of the mean, using Tukey's test. CK:  
 313 control, P1: 25 kg P ha<sup>-1</sup>, P2: 50 kg P ha<sup>-1</sup>, P3: 100 kg P ha<sup>-1</sup>.

314





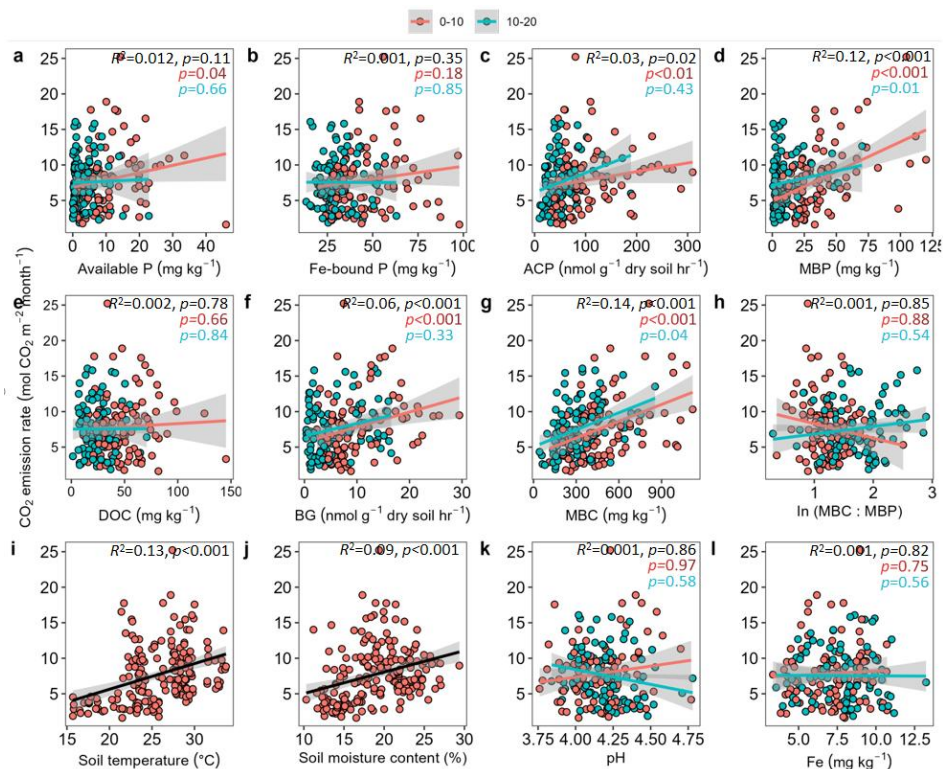
315 **3.2. Relationships between carbon fractions, enzymes, and soil properties**

316 Linear regression analysis revealed a positive increase in DOC with available  
317 P concentrations ( $p<0.001$ ) (Fig. S5a). There was also an increase in DOC as Fe-  
318 bound P increased ( $p<0.001$ ) (Fig. S5b). The concentration of DOC had a positive  
319 significant relationship ( $p<0.001$ ) with the concentration of acid phosphatase (Fig.  
320 S5c), MBP (Fig. S4d), and beta-glucosidase activity (Fig. S5e). Similarly, DOC  
321 increased with MBC ( $p=0.001$ ) (Fig. S5f) but significantly decreased ( $p<0.001$ ) with  
322 the ratio of MBC:MBP (Fig. S5g). However, the concentration of DOC was not  
323 significantly altered by the amount of crystalline Fe in the soil (Fig. S5h). DOC  
324 concentration was significantly induced by an increase in soil temperature ( $p<0.001$ )  
325 (Fig. S5i) but not soil water content ( $p=0.16$ ) (Fig. S5j), soil pH ( $p=0.59$ ) or amount  
326 of Fe in the soil ( $p=0.29$ ) (Fig. S5k).

327 Due to the distinct variation in soil microbial processes in the top (0-10 cm)  
328 and sub-soil (10-20 cm), we modeled the relationships between CO<sub>2</sub> emission and soil  
329 properties among the two soil depths using bivariate linear modeling. Unlike the  
330 concentration of DOC, the increase in CO<sub>2</sub> emission with increased available P and  
331 acid phosphatase activity was only significant in the topsoil ( $p=0.04$  and  $p<0.01$ ,  
332 respectively) (Fig. 4a and c). However, CO<sub>2</sub> emission significantly increased with  
333 increasing concentration of microbial biomass P in both soil depths ( $p<0.001$ ) (Fig.  
334 4d). The amount of CO<sub>2</sub> emitted was not significantly related to the DOC  
335 concentration ( $p=0.78$ ) (Fig. 4e), while significantly related to beta-glucosidase  
336 activity and MBC ( $p<0.001$ ) (Fig. 4f and g). Moreover, the amount of CO<sub>2</sub> emitted  
337 reveals a nonsignificantly decreasing trend with increasing MBC:MBP ratio in the  
338 topsoil and assumed the opposite direction in the subsoil (Fig. 4h). CO<sub>2</sub> emission  
339 significantly increased with soil temperature and moisture ( $p<0.001$ ) (Fig. 4i and j)



340 but was insignificantly altered soil pH and crystalline Fe concentration ( $p=0.86$ , and  
 341  $p=0.82$ , respectively) (Fig. 4k and l).

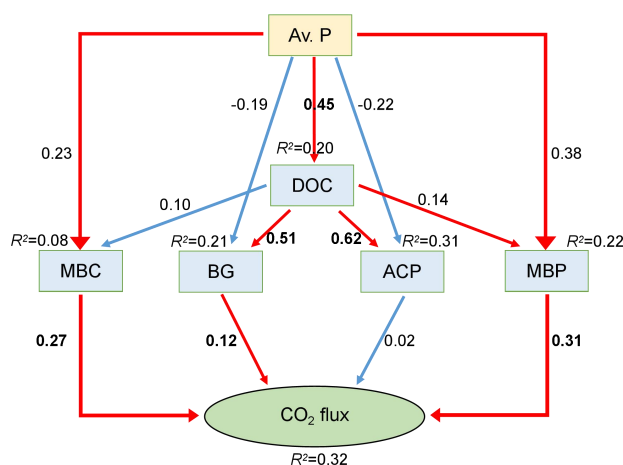


342  
 343  
 344 **Fig. 4.** Linear regression modeling showing the relationships between CO<sub>2</sub> emission  
 345 rate and soil phosphorus (P) and C fractions across the 0-10 and 10-20cm soil depth.  
 346 ACP: acid phosphatase, BG: beta-glucosidase, DOC: dissolved organic C, MBC:  
 347 microbial biomass C, MBP: microbial biomass P, Fe: iron.

348



349 To establish the key regulators of DOC and CO<sub>2</sub> flux following P addition, our  
350 SEM analysis indicated a positive relationship between available P and DOC ( $r=0.45$ ),  
351 MBP ( $r=0.38$ ), and MBC ( $r=0.23$ ) (Fig. 5). Notably, a negative association between  
352 available P and beta-glucosidase activity ( $r=-0.19$ ) and acid phosphatase ( $r=-0.22$ )  
353 was obtained (Fig. 5). On the other hand, positive relationships between DOC and  
354 MBC ( $r=0.10$ ), MBP ( $r=0.14$ ), beta-glucosidase activity ( $r=0.51$ ), and acid  
355 phosphatase ( $r=0.62$ ) were observed. The CO<sub>2</sub> emission rate was mainly positively  
356 influenced by MBP ( $r=0.31$ ), MBC ( $r=0.27$ ), beta-glucosidase activity ( $r=0.12$ ), and  
357 acid phosphatase activity ( $r=0.02$ ).  
358



359 **Fig. 5.** Structural equation modeling showing the cascading effect of P availability on  
360 carbon and phosphorus components regulating CO<sub>2</sub> flux. The red lines indicate  
361 significantly positive interaction ( $p < 0.05$ ). Av. P: available phosphorus, Fe-P: iron-  
362 bound phosphorus, ACP: acid phosphatase, MBP: microbial biomass phosphorus,  
363 MBC: microbial biomass carbon, BG: beta-glucosidase.  
364  
365



### 366 **3.3. Responses of microbial functional genes to increasing phosphorus supplies**

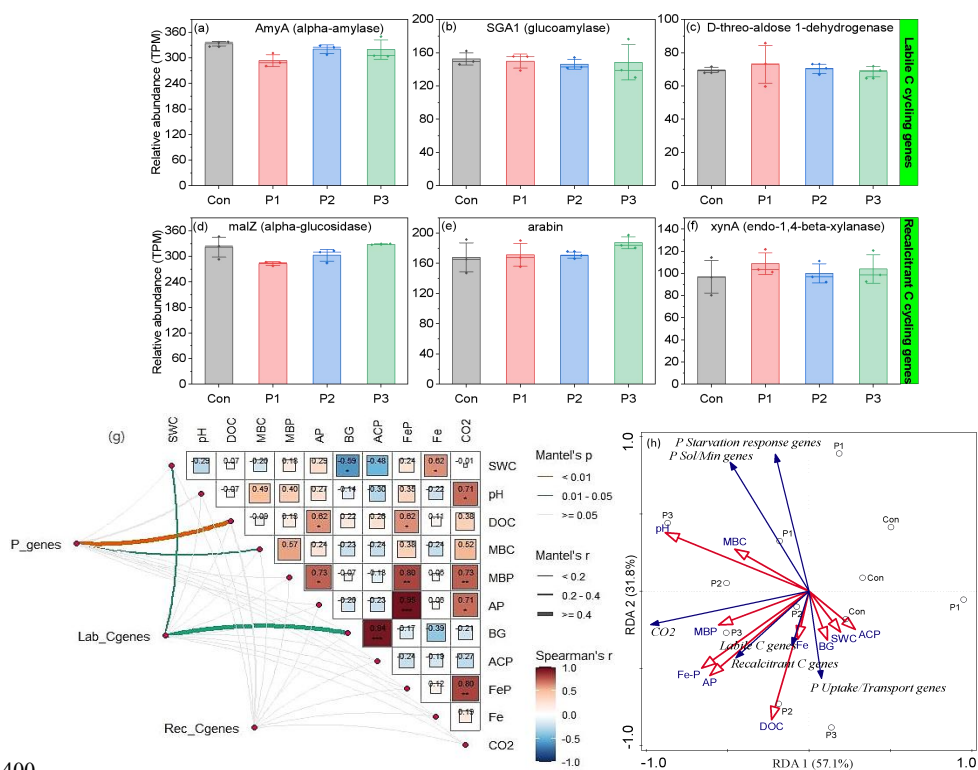
367 Our study shows that P addition did not alter the alpha diversity indices of the  
368 total functional genes knockout (KO) read numbers. The species richness of  
369 functional genes KO number represented by the Observed species (Sobs), Chao1, and  
370 Abundance-based Coverage Estimator (ACE) did not significantly vary across the P  
371 addition treatments (Fig. S6a). Also, the Shannon index, which is more sensitive to  
372 rare species, and the Simpson index, which is more sensitive to dominant species, did  
373 not significantly vary with P supplies compared to the control ( $p=0.75$  and  $0.99$ ,  
374 respectively) (Fig. S6b).

375 Three functional gene KOs with high relative abundance (transcript per  
376 million) among the vast pools of C-cycling genes were selected and evaluated. The  
377 functional genes KOs representing labile C degradation (alpha-amylase, glucoamylase,  
378 and D-threo-aldose 1-dehydrogenase) did not significantly vary due to P addition (Fig.  
379 6a-c). Similarly, those involved in recalcitrant C degradation (alpha-glucosidase,  
380 arabin and endo-1,4-betaxylanase) did not significantly differ among the treatments  
381 (Fig. 6d-f). Also, three genes with high relative abundances among the functional  
382 genes regulating P starvation responses, uptake, transport, solubilization, and  
383 mineralization were selected based on their TPM from the pools of genes for  
384 evaluation. The functional genes KOs representing P starvation response did not  
385 significantly vary due to P addition (Fig. S7a-c). This pattern also applied to the P  
386 uptake and transport genes (Fig. S7d-f) and the P solubilization and mineralization  
387 genes (Fig. S7g-i). The Mantel test used to explore the spatial autocorrelation between  
388 soil properties, CO<sub>2</sub> emission and C and P components and their functional genes  
389 indicated a significant positive relationship between CO<sub>2</sub> emission and MBP ( $r=0.73$ ,  
390  $**p < 0.01$ ), AP ( $r=0.71$ ,  $*p < 0.05$ ), and Fe-bound P ( $r=0.80$ ,  $**p < 0.01$ ) (Fig. 6g).



391 These results support the observation in our SEM analysis on the importance of P-  
392 cycling in CO<sub>2</sub> emission (Fig. 5). Besides, the thickness of the lines connecting the  
393 nodes of the P cycling related genes and DOC ( $p < 0.05$ ) was an indication of the  
394 magnitude of the correlation between P cycling and the utilization of DOC. Similarly,  
395 the direction of ordination in the RDA revealed that MBP, Fe-P, and AP significantly  
396 influenced CO<sub>2</sub> emission compared to other variables (Fig. 6h). These relationships  
397 were strongest around the P2 and P3 treatments characterized by higher P components,  
398 and particularly related to the genes involved in P uptake and transport.

399



400  
 401  
 402 **Fig. 6.** The relative abundance of carbon (C) cycling functional gene KEGG-  
 403 orthology and their multivariate relationship with soil properties across P addition at  
 404 0-10 cm depth. a-c. relative abundance of labile C-cycling genes, d-f. relative  
 405 abundance of recalcitrant C-cycling genes, g. Mantel test showing the spatial  
 406 autocorrelation between soil properties, CO<sub>2</sub> emission and C and P components and  
 407 their functional genes, h. redundancy analysis showing how soil C and P components  
 408 accounts for the variation in CO<sub>2</sub> emission and C and P cycling genes. TPM:  
 409 transcripts per million, ACP: acid phosphatase, BG: beta-glucosidase, DOC: dissolved  
 410 organic C, MBC: microbial biomass C, MBP: microbial biomass P, Fe: iron, Fe-P:  
 411 Fe-bound P, SWC: soil water content. P Sol/Min genes: P  
 412 solubilization/Mineralization genes, P\_genes: P-cycling genes, Lab\_C genes: labile C-  
 413 cycling genes, Rec\_C\_genes: recalcitrant C-cycling genes. CK: control, P1: 25 kg P ha<sup>-1</sup>,  
 414 P2: 50 kg P ha<sup>-1</sup>, P3: 100 kg P ha<sup>-1</sup>.

415

416



## 417 **4. Discussion**

### 418 ***4.1. Responses of soil phosphorus and carbon components to phosphorus supply***

419           The increase in available P across the soils with increasing application rate is  
420 relevant for exploring its effect on the dynamics of organic C. Our observed increase  
421 in the Fe-bound inorganic P with increasing P concentration agrees with our first  
422 hypothesis that in acidic conditions, increasing P availability increases Fe-bound P  
423 concentrations following the potential desorption of the organic C previously  
424 associated with Fe. This is confirmed by the consistent increasing trend in the  
425 concentration of non-crystalline Fe, potentially released following organic C  
426 desorption with increasing P addition levels (Fig. S3a-d). The binding of organic C to  
427 Fe is a key SOC stabilization pathway in acidic soils (Zhao et al., 2016; Chen et al.,  
428 2020). Under acid-to-neutral conditions, phosphate anions in soil sorbs to positively  
429 charged surfaces, such as oxides and hydroxides of Fe and Al, and positively charged  
430 binding sites on organic matter and at the edges of phyllosilicates (Hinsinger, 2001).  
431 The phosphate ions in soil possess a higher affinity for binding sites than several  
432 organic C compounds (Guppy et al., 2005; Ruttenberg and Sulak, 2011; Du et al.,  
433 2022) and could undergo anion exchange with the organic C sorbed to the soil solid  
434 phase. This high affinity of P for Fe becomes an obstacle to the formation and stability  
435 of organic C complexes (Du et al., 2022). Therefore, the increase in DOC in the  
436 topsoil across sampling times and cumulatively following P addition, particularly at  
437 higher P rates, could be associated with increasing desorption of organic C. It was  
438 previously demonstrated that only one hour after adding inorganic P, an increase of  
439 1.6-3.5 factors of DOC concentration was recorded across four soil horizons (Spohn  
440 and Schleuss, 2019). The long-term addition of inorganic P increased the  
441 concentration of DOC in tropical soils (Neff et al., 2000) and induced the dissolution



442 of organic acids (Afif et al., 1995). Also, adding P to temperate forest soils prevented  
443 the sorption of DOC to the soil solid phase (Schneider et al., 2010) and in different  
444 soil types (Spohn et al., 2022). To verify that the increase in DOC concentration was  
445 not influenced by factors such as litterfall amount or surface litter DOC concentration,  
446 our measurements showed an insignificant variation of litterfall amount and surface  
447 litter DOC among the treatments (Fig. 2c, d). This observation indicates that the  
448 interaction of Fe-OC-P mainly induced the increase in DOC with P addition via the  
449 competitive adsorption mechanism earlier hypothesized. Therefore, the amount of  
450 DOC introduced by the surface litter across the treatments did not influence the  
451 dynamic concentration of DOC with P supply in the soil system.

452 Our study showed that soil microbes did not invest in enzymatic activity that  
453 further degraded SOC following P addition. With the increase in DOC following P  
454 addition, a significant reduction in beta-glucosidase activity was involved in the  
455 breakdown of organic C to release glucose for microbial use. This observation is  
456 further supported by the fact that there was no significant change in the activity of C-  
457 degrading functional genes after P-addition. Previous studies have similarly reported  
458 that when adequate inorganic P is supplied, it could inhibit SOC decomposition in  
459 tropical forest soils (Schulze et al., 2000; Zhang et al., 2022) because soil microbes  
460 will decrease the investment in enzymes and, thus, reduce the decomposition of  
461 organic matter (Zheng et al., 2015). Furthermore, the insignificant effect of the P  
462 addition rate on soil MBC across the 0-10 and 10-20 cm depths indicates microbial  
463 utilization of most of the excess DOC for other metabolic processes at the expense of  
464 its incorporation as MBC. However, MBP increased with increasing DOC  
465 concentration, indicating greater allocation of the released labile C into building MBP,  
466 a process that requires an enormous amount of C. Similar observations of the





467 insignificant effect of inorganic P addition on soil MBC have been previously  
468 documented (Spohn and Schleuss, 2019; Spohn et al., 2022), even across different soil  
469 profiles (Heuck et al., 2015). In contrast, some studies reported increased soil MBC  
470 from the long-term addition of P to grasslands (Griffiths et al., 2012; Chen et al., 2014)  
471 and in mature tropical forests in the subtropical region of China (Liu et al., 2012).  
472 Similarly, soil MBC increased after long-term P addition in a lowland tropical forest  
473 (Turner and Joseph Wright, 2014). While these authors posit that the increase in MBC  
474 following P addition was due to the alleviation of P limitation in microbial biomass,  
475 the results from our study, however, provide an alternative mechanism that the  
476 desorbed organic C was utilized as C source for incorporating the added P into  
477 microbial biomass at the expense of MBC; hence, the insignificant change in MBC  
478 recorded in our study.

479         With increasing P supplies, soil DOC increased and was associated with a  
480 consistent increase in CO<sub>2</sub> flux, particularly at higher P supply rates (P2 and P3) (Fig.  
481 3e). This indicates the capacity of the desorbed organic C to provide sufficient labile  
482 C required for increasing microbial metabolism and respiration. Our finding of  
483 increased respiration following P addition agrees with previous studies reporting  
484 increased soil respiration due to inorganic P addition (Cleveland et al., 2002; Fisk et  
485 al., 2015; Liu et al., 2012; Spohn and Schleuss, 2019; Munevar and Wollum, 1977).  
486 The increase in respiration after P addition in these studies was attributed to the  
487 alleviation of microbial P limitation. However, our investigation revealed that C  
488 limitation was induced due to the high amount of C needed for incorporating the  
489 added P into microbial biomass. Thus, DOC was increasingly utilised as the primary  
490 microbial C source, further inducing respiration. The building of MBP requires  
491 significant utilization of enormous labile organic C to execute, thus substantially



492 increasing microbial respiration with increasing P availability. Generally, when there  
493 is an excess of available soil P, microbes can utilize this P more efficiently if there is  
494 an adequate supply of readily available organic C (Fanin et al., 2015). Thus, the  
495 desorbed C due to P supply provided the energy and the necessary building blocks for  
496 microbial growth and incorporation of excess P into biomass, a process that  
497 contributed to the increased CO<sub>2</sub> recorded. If the DOC availability is limited, the  
498 ability of microbes to utilize and incorporate the excess soil P into their biomass may  
499 be reduced. Microbial C limitation has been shown to induce a lag effect of P addition  
500 on soil microbial biomass in the initial years following P addition (Liu et al., 2015).  
501 Therefore, our study provides newer insights that the desorbed C alleviated microbial  
502 C limitation to drive the incorporation of P into microbial biomass to further induce  
503 CO<sub>2</sub> emission in P-amended soils.

#### 504 ***4.2. Relationships between carbon and phosphorus components***

505 The significant positive relationship between DOC, available P, and Fe-bound  
506 P concentrations in our linear regression model supports our hypothesis of the  
507 preferential sorption of free Fe desorbed from the Fe-OC interface to P (Xia et al.,  
508 2024; Spohn et al., 2022). Besides, the positive relationships between acid  
509 phosphatase and MBP with DOC concentration are consistent with the fact that the  
510 amount of DOC in soil determines the capacity of microbes to utilize and incorporate  
511 excess available P into microbial biomass effectively. However, we observed that  
512 higher CO<sub>2</sub> emission, particularly in the topsoil, only occurs when MBP incorporation  
513 exceeds MBC. This is because an enormous C is required for incorporating P into  
514 microbial biomass, which is the key regulator of CO<sub>2</sub> emission under P addition. Our  
515 reports agree with the conclusions of Heuck et al. (2015), who reported that the



516 microbial biomass possesses higher C limitation but is not limited by N or P when P  
517 is available. Our linear regression model further shows significant positive increases  
518 in  $\beta$ -glucosidase and MBC with DOC, indicating the capacity of microbes to utilize  
519 and incorporate the excess labile C into the microbial biomass. However, a negative  
520 relationship ensued between DOC and the MBC:MBP ratio, indicating that the labile  
521 organic C was preferentially used for building MBP instead of MBC. However, the  
522 concentration of DOC was not significantly related to the amount of crystalline Fe in  
523 the soil (Fig. S4k), indicating that most of the free Fe in the soil was increasingly  
524 associated with P after the desorption of Fe-bound organic C.

525 Our observed positive linear relationship between available P in the topsoil  
526 and CO<sub>2</sub> emission agrees with the increased soil respiration due to inorganic P  
527 addition previously reported (Cleveland et al., 2002; Fisk et al., 2015; Liu et al., 2012;  
528 Spohn and Schleuss, 2019; Cleveland and Townsend, 2006). While the amount of  
529 CO<sub>2</sub> emitted increased with MBC and MBP, it showed a decreasing trend with a  
530 higher MBC:MBP ratio. This finding implies that higher incorporation of P into  
531 microbial biomass relative to C drives CO<sub>2</sub> emission. Taken together, the increase in  
532 CO<sub>2</sub> emission upon inorganic P addition is primarily a consequence of the  
533 incorporation of P into microbial biomass, a process that requires enormous labile C.  
534 Previous studies have often concluded that the stimulation of soil CO<sub>2</sub> efflux due to  
535 the addition of inorganic P is due to the removal of microbial P limitation and the  
536 stimulation of microbial activity (Cleveland et al., 2002; Fisk et al., 2015; Liu et al.,  
537 2012; Spohn and Schleuss, 2019). However, our results provided an alternative  
538 mechanism that C-limitation is induced during microbial incorporation of excess P  
539 into biomass and that the desorbed organic C is quickly metabolized by soil  
540 microorganisms, thus inducing CO<sub>2</sub> emission. CO<sub>2</sub> emission was further stimulated



541 during periods with higher soil temperature and a relative increase in soil moisture to  
542 support microbial activities. CO<sub>2</sub> emission increases with increasing soil temperature  
543 (Natali et al., 2015). While excess soil moisture could limit CO<sub>2</sub> emission (Ibrahim et  
544 al., 2022), increasing soil moisture to a sufficient level could promote microbial  
545 activities and drive respiration. Seasonal transition from wet to dry drove an 18%  
546 annual increase in CO<sub>2</sub> emission from the P-fertilized plots (Cleveland and Townsend,  
547 2006), indicating the key role of soil moisture in regulating CO<sub>2</sub>.

548 The SEM analysis revealed that the amount of DOC indirectly influenced CO<sub>2</sub>  
549 emission due to its role in sustaining the immediate labile C requirement for microbial  
550 activities. The significantly positive relationship between CO<sub>2</sub> emission, acid  
551 phosphatase, and MBP compared to beta-glucosidase and MBC indicated that  
552 microbial utilization of DOC as an energy source for P cycling and mobilization into  
553 biomass was the dominant regulator of CO<sub>2</sub> emission. Compared to beta-glucosidase  
554 activity, the stronger positive relationship between DOC and acid phosphatase  
555 buttresses our observation of its higher utilization for P cycling. Despite these  
556 observations, it was evident that C-cycling also significantly contributed to CO<sub>2</sub>  
557 emission.

#### 558 ***4.3. Responses of microbial functional genes to increasing phosphorus supplies***

559 Microbial gene KO read numbers are a powerful tool for studying gene  
560 function and exploring how specific genes in microorganisms regulate soil processes.  
561 We show no alteration of the alpha diversity indices of total functional genes KOs to  
562 P addition. We show that P supplies had insignificant effects on the relative  
563 abundances of the functional genes KOs representing labile and recalcitrant C  
564 degradation (Fig. 6a-f). This result suggests that the labile C needed for immediate



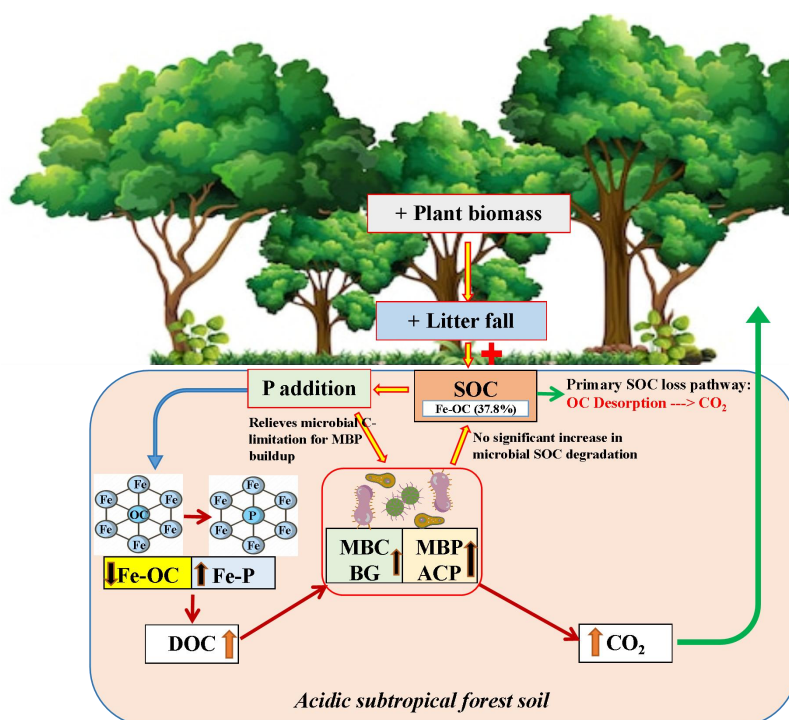
565 microbial use was not limiting, and the degradation of further SOC was not prioritized.  
566 These results infer that the desorbed organic C due to P addition was available to  
567 sustain microbial C limitation needed to drive microbial metabolic processes.  
568 Previous reports have indicated that P addition promoted SOC decomposition by  
569 stimulating C-cycling-related genes, with a greater effect on the abundance of  
570 recalcitrant C-degrading genes than labile C-degrading genes in saline-sodic soils (Du  
571 et al., 2023), and in alpine meadow (Ye et al., 2023).

572 Our hypothesis that P cycling significantly contributed to CO<sub>2</sub> emission was  
573 further verified by multivariate analyses using the spatial autocorrelation of the  
574 Mantel test (Fig. 6g). Similarly, the multivariate RDA supports our hypothesis by  
575 indicating the proximity, the low acute angle, and the length of arrows of cluster  
576 points of CO<sub>2</sub>, MBP, Fe-bound P, available P, and DOC compared to other variables  
577 (Fig 6g). P-cycling requires enormous C to meet microbial energy needs (Heuck et al.,  
578 2015). Besides, the strong autocorrelation between P-cycling genes and DOC in the  
579 Mantel test was further clarified in the RDA, where an acute angle between CO<sub>2</sub>  
580 emission rate and microbial genes involved in P uptake and transport ensued. These  
581 results further support our earlier observation that the incorporation of MBP and the  
582 roles of genes involved in P uptake and transport significantly drive CO<sub>2</sub> emission.  
583 Even though P addition results in the degradation of SOC (Ye et al., 2023; Du et al.,  
584 2023), the microbial C need for further P-cycling could have stimulated this process.  
585 Therefore, we alternatively propose that the desorbed organic C following P addition  
586 in acidic forest soil was sufficient to meet microbial P requirement without  
587 significantly degradation SOC for their C needs.

588 A key implication of the study is that C loss as CO<sub>2</sub> could be potentially  
589 higher in acidic subtropical forests, soil rich in Fe, and regions of higher P availability.



590 Therefore, a trade-off exists between SOC accumulation from the potential increase in  
591 plant biomass (resulting from higher litterfall and SOC accumulation) in regions of  
592 higher P and the amount lost via increased CO<sub>2</sub> emission. This could undermine the  
593 overall subtropical forest C storage potential if the amount of litter-derived organic C  
594 does not exceed the amount of desorbed organic C because we revealed that the  
595 excess DOC was not leached down the soil for deep storage. Following our results,  
596 we reconstructed the framework for the processes occurring in acidic subtropical  
597 forest soil following P supplies in Figure 7.



598  
599 **Fig. 7.** A framework of the effect of phosphorus (P) addition on soil organic carbon  
600 (SOC) stability from the study. P addition induces the desorption of Fe-bound organic  
601 C to increase DOC. The DOC serves as the key microbial C source for enzymatic  
602 activities and incorporating P and C into microbial biomass. The enormous C required  
603 for MBP incorporation drives CO<sub>2</sub> emission at a faster rate than the C required for  
604 MBC.  
605



606           While our study provided an innovative and alternative mechanism on how P  
607 supplies influence C cycling and CO<sub>2</sub> emission from subtropical forest soils, some  
608 limitations still exist in our explorations. First, our study was limited to one forest  
609 type, and samplings were carried out periodically over one year. Thus, how the  
610 mechanisms reported here fluctuate in the long-term following continuous P addition  
611 remains uncertain. Second, our study focused on the one-time application of P rates  
612 per year and measuring the impulse response pattern of SOC, unlike the continuous  
613 replenishment strategy used in some instances. Besides, our findings and conclusions  
614 are limited to acidic subtropical forest soil rich in Fe and capable of binding anions.  
615 Thus, these findings would require validation before they can be extrapolated to other  
616 soil ecosystems. Despite these limitations, we have provided important alternative  
617 mechanisms for understanding and predicting the alterations in SOC subtropical forest  
618 soils. Future research should consider integrating the roles of climate, soil type, and  
619 structure, forest types, tree species diversity, and soil nutrient interactions (and their  
620 spatial distribution) on the alteration of SOC under acidic conditions.

## 621 **5. Conclusion**

622           Our study supports our hypothesis that the availability of inorganic P in acidic  
623 subtropical forest soil increases soil DOC by promoting the formation of Fe-bound P  
624 following the desorbing organic C previously bound to Fe. Increased microbial  
625 respiration was stimulated following P addition because the desorbed organic C was  
626 mainly utilized to relieve microbial C limitation, which was induced following the  
627 incorporation of P into the microbial biomass. Thus, CO<sub>2</sub> emission was significantly  
628 stimulated, especially with increasing MBP. The microbial utilization of desorbed C  
629 for MBP build-up was the most significant factor in regulating CO<sub>2</sub> emission.  
630 Moreover, the non-significant change in microbial C-degrading enzymes and the



631 relative abundance of C-degrading functional genes indicates that the microbial C  
632 source was primarily derived from freshly desorbed C rather than further microbial  
633 degradation of SOC. Our study highlights newer and alternative mechanisms into how  
634 P addition influences CO<sub>2</sub> emission and SOC dynamics in acidic soils, which is vital  
635 for understanding the fate of SOC across P concentration gradients in subtropical  
636 forests.

#### 637 **CRedit authorship contribution statement**

638 JT: Investigation, Methodology, Software, Writing - review & editing. MMI:  
639 Conceptualization, Data curation, Formal analysis, Investigation, Methodology,  
640 Software, Funding acquisition, Writing - original draft, Writing - review & editing.  
641 HL: Conceptualization, Investigation, Methodology. ZC: Investigation, Methodology.  
642 CG: Investigation, Methodology. ZL: Investigation, Methodology. XL: Investigation,  
643 Methodology. YL: Investigation, Methodology. EH: Conceptualization, Investigation,  
644 Methodology, Data curation, Funding acquisition, Supervision, Validation,  
645 Visualization, Writing- review & editing, Project administration, Resources.

#### 646 **Acknowledgments**

647 This work was supported by the National Natural Science Foundation of China  
648 (W2433082; 32322054, 32271644), China Postdoctoral Science Foundation  
649 (2023M743544), and the Guangdong Basic and Applied Basic Research Foundation  
650 (2022B1515020014).

#### 651 **Data availability**

652 The data supporting the findings of this study are openly available in "Figshare" at  
653 <https://doi.org/10.6084/m9.figshare.28122539>.





654 **Conflict of interest statement**

655 The authors declare that they have no known competing financial interests or personal  
656 relationships that could have appeared to influence the work reported in this article.

657

658 **References**

- 659 Afif, E., Barrón, V., and Torrent, J.: Organic matter delays but does not prevent  
660 phosphate sorption by Cerrado soils from Brazil, *Soil Science*, 159, 207-211,  
661 1995.
- 662 Bell, C. W., Fricks, B. E., Rocca, J. D., Steinweg, J. M., McMahon, S. K., and  
663 Wallenstein, M. D.: High-throughput fluorometric measurement of potential  
664 soil extracellular enzyme activities, *JoVE (Journal of Visualized Experiments)*,  
665 e50961, 2013.
- 666 Chen, C., Hall, S. J., Coward, E., and Thompson, A.: Iron-mediated organic matter  
667 decomposition in humid soils can counteract protection, *Nature*  
668 *Communications*, 11, 2255, 2020.
- 669 Chen, J., Hu, Y., Hall, S. J., Hui, D., Li, J., Chen, G., Sun, L., Zhang, D., and Deng,  
670 Q.: Increased interactions between iron oxides and organic carbon under acid  
671 deposition drive large increases in soil organic carbon in a tropical forest in  
672 southern China, *Biogeochemistry*, 158, 287-301, 2022.
- 673 Chen, X., Daniell, T. J., Neilson, R., O'Flaherty, V., and Griffiths, B. S.: Microbial  
674 and microfaunal communities in phosphorus limited, grazed grassland change  
675 composition but maintain homeostatic nutrient stoichiometry, *Soil Biology*  
676 *and Biochemistry*, 75, 94-101, 2014.
- 677 Cleveland, C. C. and Townsend, A. R.: Nutrient additions to a tropical rain forest  
678 drive substantial soil carbon dioxide losses to the atmosphere, *Proceedings of*  
679 *the National Academy of Sciences*, 103, 10316-10321, 2006.
- 680 Cleveland, C. C., Townsend, A. R., and Schmidt, S. K.: Phosphorus limitation of  
681 microbial processes in moist tropical forests: evidence from short-term  
682 laboratory incubations and field studies, *Ecosystems*, 5, 0680-0691, 2002.



- 683 Du, J., Liu, K., Huang, J., Han, T., Zhang, L., Anthonio, C. K., Shah, A., Khan, M. N.,  
684 Qaswar, M., and Abbas, M.: Organic carbon distribution and soil aggregate  
685 stability in response to long-term phosphorus addition in different land-use  
686 types, *Soil and Tillage Research*, 215, 105195, 2022.
- 687 Du, X., Ge, Y., Zhang, Y., Hu, H., Zhang, Y., Yang, Z., Ren, X., Hu, S., Feng, H.,  
688 and Song, Y.: Responses of soil carbon cycling microbial functional genes to  
689 nitrogen and phosphorus addition in saline-sodic soils, *Plant and Soil*, 490,  
690 261-277, 10.1007/s11104-023-06070-y, 2023.
- 691 Fang, X.-M., Zhang, X.-L., Chen, F.-S., Zong, Y.-Y., Bu, W.-S., Wan, S.-Z., Luo, Y.,  
692 and Wang, H.: Phosphorus addition alters the response of soil organic carbon  
693 decomposition to nitrogen deposition in a subtropical forest, *Soil Biology and  
694 Biochemistry*, 133, 119-128, 2019.
- 695 Fanin, N., Hättenschwiler, S., Schimann, H., and Fromin, N.: Interactive effects of C,  
696 N and P fertilization on soil microbial community structure and function in an  
697 Amazonian rain forest, *Functional Ecology*, 29, 140-150, 2015.
- 698 Fisk, M., Santangelo, S., and Minick, K.: Carbon mineralization is promoted by  
699 phosphorus and reduced by nitrogen addition in the organic horizon of  
700 northern hardwood forests, *Soil Biology and Biochemistry*, 81, 212-218, 2015.
- 701 Griffiths, B. S., Spilles, A., and Bonkowski, M.: C: N: P stoichiometry and nutrient  
702 limitation of the soil microbial biomass in a grazed grassland site under  
703 experimental P limitation or excess, *Ecological Processes*, 1, 1-11, 2012.
- 704 Guppy, C. N., Menzies, N. W., Moody, P. W., and Blamey, F. P. C.: Competitive  
705 sorption reactions between phosphorus and organic matter in soil: a review,  
706 *Soil Research*, 43, 189-202, 2005.
- 707 Harris, N. L., Gibbs, D. A., Baccini, A., Birdsey, R. A., De Bruin, S., Farina, M.,  
708 Fatoyinbo, L., Hansen, M. C., Herold, M., and Houghton, R. A.: Global maps  
709 of twenty-first century forest carbon fluxes, *Nature Climate Change*, 11, 234-  
710 240, 2021.
- 711 He, X., Augusto, L., Goll, D. S., Ringeval, B., Wang, Y., Helfenstein, J., Huang, Y.,  
712 Yu, K., Wang, Z., and Yang, Y.: Global patterns and drivers of soil total  
713 phosphorus concentration, *Earth System Science Data Discussions*, 2021, 1-21,  
714 2021.



- 715 Heuck, C., Weig, A., and Spohn, M.: Soil microbial biomass C: N: P stoichiometry  
716 and microbial use of organic phosphorus, *Soil Biology and Biochemistry*, 85,  
717 119-129, 2015.
- 718 Hinsinger, P.: Bioavailability of soil inorganic P in the rhizosphere as affected by  
719 root-induced chemical changes: a review, *Plant and soil*, 237, 173-195, 2001.
- 720 Hou, E., Chen, C., Wen, D., and Liu, X.: Relationships of phosphorus fractions to  
721 organic carbon content in surface soils in mature subtropical forests,  
722 Dinghushan, China, *Soil Research*, 52, 55-63, 2014.
- 723 Hou, E., Tang, S., Chen, C., Kuang, Y., Lu, X., Heenan, M., and Wen, D.: Solubility  
724 of phosphorus in subtropical forest soils as influenced by low-molecular  
725 organic acids and key soil properties, *Geoderma*, 313, 172-180, 2018.
- 726 Hou, E., Wen, D., Jiang, L., Luo, X., Kuang, Y., Lu, X., Chen, C., Allen, K. T., He,  
727 X., and Huang, X.: Latitudinal patterns of terrestrial phosphorus limitation  
728 over the globe, *Ecology Letters*, 24, 1420-1431, 2021.
- 729 Ibrahim, M. M., Guo, L., Wu, F., Liu, D., Zhang, H., Zou, S., Xing, S., and Mao, Y.:  
730 Field-applied biochar-based MgO and sepiolite composites possess CO<sub>2</sub>  
731 capture potential and alter organic C mineralization and C-cycling bacterial  
732 structure in fertilized soils, *Science of the Total Environment*, 813, 152495,  
733 2022.
- 734 Li, D., Liu, C. M., Luo, R., Sadakane, K., and Lam, T. W.: MEGAHIT: an ultra-fast  
735 single-node solution for large and complex metagenomics assembly via  
736 succinct de Bruijn graph, *Bioinformatics (Oxford, England)*, 31, 1674-1676,  
737 10.1093/bioinformatics/btv033, 2015.
- 738 Liu, F., Wang, D., Zhang, B., and Huang, J.: Concentration and biodegradability of  
739 dissolved organic carbon derived from soils: A global perspective, *Science of  
740 the Total Environment*, 754, 142378, 2021.
- 741 Liu, L., Gundersen, P., Zhang, T., and Mo, J.: Effects of phosphorus addition on soil  
742 microbial biomass and community composition in three forest types in tropical  
743 China, *Soil Biology and Biochemistry*, 44, 31-38, 2012.
- 744 Liu, L., Gundersen, P., Zhang, W., Zhang, T., Chen, H., and Mo, J.: Effects of  
745 nitrogen and phosphorus additions on soil microbial biomass and community  
746 structure in two reforested tropical forests, *Scientific Reports*, 5, 14378,  
747 10.1038/srep14378, 2015.



- 748 Munevar, F. and Wollum, A. G.: Effects of the addition of phosphorus and inorganic  
749 nitrogen on carbon and nitrogen mineralization in Andepts from Colombia,  
750 Soil Science Society of America Journal, 41, 540-545, 1977.
- 751 Natali, S. M., Schuur, E. A. G., Mauritz, M., Schade, J. D., Celis, G., Crummer, K. G.,  
752 Johnston, C., Krapek, J., Pegoraro, E., and Salmon, V. G.: Permafrost thaw  
753 and soil moisture driving CO<sub>2</sub> and CH<sub>4</sub> release from upland tundra, Journal of  
754 Geophysical Research: Biogeosciences, 120, 525-537, 2015.
- 755 Neff, J. C., Hobbie, S. E., and Vitousek, P. M.: Nutrient and mineralogical control on  
756 dissolved organic C, N and P fluxes and stoichiometry in Hawaiian soils,  
757 Biogeochemistry, 51, 283-302, 2000.
- 758 Ohno, T. and Zibilske, L. M.: Determination of Low Concentrations of Phosphorus in  
759 Soil Extracts Using Malachite Green, Soil Science Society of America Journal,  
760 55, 892-895, 1991.
- 761 Ruttenberg, K. C. and Sulak, D. J.: Sorption and desorption of dissolved organic  
762 phosphorus onto iron (oxyhydr) oxides in seawater, Geochimica et  
763 Cosmochimica Acta, 75, 4095-4112, 2011.
- 764 Schneider, M. P. W., Scheel, T., Mikutta, R., Van Hees, P., Kaiser, K., and Kalbitz,  
765 K.: Sorptive stabilization of organic matter by amorphous Al hydroxide,  
766 Geochimica et Cosmochimica Acta, 74, 1606-1619, 2010.
- 767 Schulze, E. D., Högberg, P., Van Oene, H., Persson, T., Harrison, A. F., Read, D.,  
768 Kjøller, A., and Matteucci, G.: Interactions between the carbon and nitrogen  
769 cycles and the role of biodiversity: a synopsis of a study along a north-south  
770 transect through Europe, in: Carbon and nitrogen cycling in European forest  
771 ecosystems, Springer, 468-491, 2000.
- 772 Slessarev, E. W., Mayer, A., Kelly, C., Georgiou, K., Pett-Ridge, J., and Nuccio, E. E.:  
773 Initial soil organic carbon stocks govern changes in soil carbon: Reality or  
774 artifact?, Global Change Biology, 29, 1239-1247, 2023.
- 775 Spohn, M. and Schleuss, P.-M.: Addition of inorganic phosphorus to soil leads to  
776 desorption of organic compounds and thus to increased soil respiration, Soil  
777 Biology and Biochemistry, 130, 220-226, 2019.
- 778 Spohn, M., Diáková, K., Aburto, F., Doetterl, S., and Borovec, J.: Sorption and  
779 desorption of organic matter in soils as affected by phosphate, Geoderma, 405,  
780 115377, 2022.



- 781 Tiwari, T., Sponseller, R. A., and Laudon, H.: The emerging role of drought as a  
782 regulator of dissolved organic carbon in boreal landscapes, *Nature*  
783 *Communications*, 13, 5125, 2022.
- 784 Trumbore, S.: Carbon respired by terrestrial ecosystems—recent progress and  
785 challenges, *Global Change Biology*, 12, 141-153, 2006.
- 786 Turner, B. L. and Joseph Wright, S.: The response of microbial biomass and  
787 hydrolytic enzymes to a decade of nitrogen, phosphorus, and potassium  
788 addition in a lowland tropical rain forest, *Biogeochemistry*, 117, 115-130,  
789 2014.
- 790 Vance, E. D., Brookes, P. C., and Jenkinson, D. S.: An extraction method for  
791 measuring soil microbial biomass C, *Soil biology and Biochemistry*, 19, 703-  
792 707, 1987.
- 793 Wordofa, D. N., Adhikari, D., Dunham-Cheatham, S. M., Zhao, Q., Poulson, S. R.,  
794 Tang, Y., and Yang, Y.: Biogeochemical fate of ferrihydrite-model organic  
795 compound complexes during anaerobic microbial reduction, *Science of the*  
796 *total environment*, 668, 216-223, 2019.
- 797 WRI: World Resources Institute: Global Forest Review, forest-extent-indicators 2023.
- 798 Xia, Y., Peñuelas, J., Sardans, J., Zhong, X., Xu, L., Yang, Z., Yang, Y., Yang, L.,  
799 Yue, K., and Fan, Y.: Phosphorus addition accelerates soil organic carbon  
800 mineralization by desorbing organic carbon and increasing microbial activity  
801 in subtropical forest soils, *Applied Soil Ecology*, 193, 105166, 2024.
- 802 Ye, L. F., Liu, H. Y., Dan Deng, H., Zheng, Y. P., Han, Y. W., Gao, X. T., Abbott, L.  
803 K., Zhao, C. M., and Li, J. H.: Effects of decadal nitrogen and phosphorus  
804 fertilization on microbial taxonomic and functional attributes associated with  
805 soil organic carbon decomposition and concentration in an alpine meadow,  
806 *Ecological Indicators*, 146, 109790, 2023.
- 807 Zhang, J., Zhou, J., Lambers, H., Li, Y., Li, Y., Qin, G., Wang, M., Wang, J., Li, Z.,  
808 and Wang, F.: Nitrogen and phosphorus addition exerted different influences  
809 on litter and soil carbon release in a tropical forest, *Science of the Total*  
810 *Environment*, 832, 155049, 2022.
- 811 Zhao, Q., Poulson, S. R., Obrist, D., Sumaila, S., Dynes, J. J., McBeth, J. M., and  
812 Yang, Y.: Iron-bound organic carbon in forest soils: quantification and  
813 characterization, *Biogeosciences*, 13, 4777-4788, 2016.



814 Zheng, M., Huang, J., Chen, H., Wang, H., and Mo, J.: Responses of soil acid  
815 phosphatase and beta-glucosidase to nitrogen and phosphorus addition in two  
816 subtropical forests in southern China, *European Journal of Soil Biology*, 68,  
817 77-84, 2015.

818 Zheng, M., Zhang, T., Luo, Y., Liu, J., Lu, X., Ye, Q., Wang, S., Huang, J., Mao, Q.,  
819 and Mo, J.: Temporal patterns of soil carbon emission in tropical forests under  
820 long-term nitrogen deposition, *Nature Geoscience*, 15, 1002-1010, 2022.

821  
822